Tomato Wall-Associated Kinase SlWak1 Depends on Fls2/Fls3 to Promote Apoplastic Immune Responses to *Pseudomonas syringae*[1[OPEN]]

Ning Zhang,[a,2] Marina A. Pombo,[b] Hernan G. Rosli,[b] and Gregory B. Martin[a,c,3]

[a]Boyce Thompson Intitute for Plant Research, Ithaca, New York 14853
[b]Instituto de Fisiología Vegetal, Universidad Nacional de La Plata, Consejo Nacional de Investigaciones Científicas y Técnicas (CONICET), La Plata, Buenos Aires, 1900 Argentina
[c]Plant Pathology and Plant-Microbe Biology Section, School of Integrative Plant Science, Cornell University, Ithaca, New York 14853

ORCID IDs: 0000-0003-2775-1755 (N.Z.); 0000-0003-4057-2700 (M.A.P.); 0000-0002-3929-5630 (H.G.R.); 0000-0003-0044-6830 (G.B.M.).

Wall-associated kinases (Waks) are important components of plant immunity against various pathogens, including the bacterium *Pseudomonas syringae* pv. tomato (*Pst*). However, the molecular mechanisms of their role(s) in plant immunity are largely unknown. In tomato (*Solanum lycopersicum*), wall-associated kinase 1 (SlWak1), has been implicated in pattern recognition receptor (PRR)-triggered immunity (PTI) because its transcript abundance increases significantly after treatment with the flagellin-derived, microbe-associated molecular patterns flg22 and flgII-28, which activate the PRRs Fls2 and Fls3, respectively. We generated two *SlWak1* tomato mutants (Δwak1) using CRISPR/Cas9 gene editing technology and investigated the role of *SlWak1* in tomato–*Pst* interactions. Late PTI responses activated in the apoplast by flg22 or flgII-28 were compromised in Δwak1 plants, but PTI at the leaf surface was unaffected. The Δwak1 plants developed fewer callose deposits than wild-type plants, but retained early PTI responses such as generation of reactive oxygen species and activation of mitogen-activated protein kinases upon exposure to flg22 and flgII-28. Induction of *Wak1* gene expression by flg22 and flgII-28 was greatly reduced in a tomato mutant lacking Fls2 and Fls3, but induction of *Fls3* gene expression by flgII-28 was unaffected in Δwak1 plants. After *Pst* inoculation, Δwak1 plants developed disease symptoms more slowly than Δfls2.1/2.2/3 mutant plants, although ultimately, both plants were similarly susceptible. SlWak1 coimmunoprecipitated with both Fls2 and Fls3, independently of flg22/flgII-28 or of BRASSINOSTEROID INSENSITIVE1-ASSOCIATED RECEPTOR KINASE1. These observations suggest that SlWak1 acts in a complex with Fls2/Fls3 and is important at later stages of PTI in the apoplast.

Plants have evolved a sophisticated, two-layered inducible defense system, consisting of pattern-recognition receptor (PRR)-triggered immunity (PTI) and nucleotide-binding Leu-rich repeat (NLR)-triggered immunity (NTI), to protect themselves against infection by pathogenic microbes (Zipfel, 2014; Bigeard et al., 2015; Lolle et al., 2020). To initiate the PTI response, host PRRs detect potential microbial pathogens by recognizing diverse microbe-associated molecular patterns (MAMPs) or pathogen-associated molecular patterns including peptides from bacterial flagellin (Boller and Felix, 2009). The resulting PTI responses include the production of reactive oxygen species (ROS), activation of mitogen-activated protein kinase (MAPK) cascades, callose deposition at the cell wall, transcriptional reprogramming of immunity-associated genes, and moderate inhibition of pathogen growth (Chandra et al., 1996; Jia and Martin, 1999; Zipfel, 2014; Li et al., 2016). Two PRRs, Flagellin-sensitive2 (Fls2) and Fls3, bind the flagellin-derived MAMPs flg22 and flgII-28, respectively, and in concert with the coreceptor BRASSINOSTEROID INSENSITIVE1-ASSOCIATED RECEPTOR KINASE1 (BAK1; in tomato [*Solanum lycopersicum*], Somatic embryogenesis receptor kinase [Serk3A and/or Serk3B]), activate intracellular immune signaling (Chinchilla et al., 2007; Sun et al., 2013; Hind et al., 2016).

To overcome PTI, pathogens deliver virulence proteins (effectors) into the plant cells to interfere with MAMP detection or PTI signaling and promote disease development (Toruño et al., 2016; Wei et al., 2018).

[1]This work is supported by the National Science Foundation (grant no. IOS–1546625 to G.B.M.) and the Agencia Nacional de Promoción Científica y Técnica – Argentina (grant no. PICT 2017–0916 to M.A.P.).

[2]Senior author.
[3]Author for contact: gbm7@cornell.edu.

The author responsible for distribution of materials integral to the findings presented in this article in accordance with the policy described in the Instructions for Authors (www.plantphysiol.org) is: Gregory B. Martin (gbm7@cornell.edu).

G.B.M. and N.Z. conceived and designed the experiments; M.A.P. and H.G.R. performed the callose deposition assay and stomata measurements; N.Z. designed gRNAs, constructed vectors, performed genotyping and phenotyping experiments, and analyzed the data; N.Z. and G.B.M. interpreted the data and wrote the article; all the authors read and approved of the article.

[OPEN]Articles can be viewed without a subscription.

www.plantphysiol.org/cgi/doi/10.1104/pp.20.00144

AvrPto and AvrPtoB, two effectors from *Pseudomonas syringae* pv. tomato (*Pst*), suppress the early PTI response by interfering with the interaction of Fls2 with BAK1 (Xiang et al., 2008; Martin, 2012; Hind et al., 2016). In response to bacterial effectors, plants have evolved genes encoding NLRs, which recognize specific effectors and activate NTI (Martin et al., 2003; Cui et al., 2015; Jubic et al., 2019; Tamborski and Krasileva, 2020). In tomato, the Pto kinase protein interacts with AvrPto or AvrPtoB and forms a complex with the NLR protein Prf resulting in the induction of NTI and inhibition of pathogen growth (Martin et al., 1993; Salmeron et al., 1996; Pedley and Martin, 2003).

Plant cell wall-associated kinases (Wak) or Wak-like kinases are receptor-like protein kinases consisting of an extracellular domain with conserved epidermal growth factor repeats, a transmembrane domain, and a cytoplasmic Ser/Thr protein kinase domain (Anderson et al., 2001). While some Wak proteins play a vital role in cell expansion and plant development (Lally et al., 2001; Wagner and Kohorn, 2001; Kohorn et al., 2006), others are expressed only in specific organs and differentially regulated by a variety of biotic or abiotic stimuli including pathogen attack (Hou et al., 2005; Li et al., 2009; Brutus et al., 2010; Hu et al., 2014; Zuo et al., 2015; Lou et al., 2019). Wak proteins have been reported to be involved in host resistance against various pathogens in plants, including Arabidopsis (*Arabidopsis thaliana*; Brutus et al., 2010), a wild species of tobacco (*Nicotiana benthamiana*; Rosli et al., 2013), rice (*Oryza sativa*; Li et al., 2009; Hu et al., 2014; Delteil et al., 2016; Harkenrider et al., 2016), maize (*Zea mays*; Hurni et al., 2015; Zuo et al., 2015; Yang et al., 2019), and wheat (*Triticum aestivum*; Yang et al., 2014; Saintenac et al., 2018; Dmochowska-Boguta et al., 2020). In one case, the wheat *Snn1*-encoded Wak protein acts as a susceptibility factor to promote infection of a fungal pathogen *Parastagonospora nodorum* (Shi et al., 2016).

Although Wak proteins have been identified as important contributors to disease resistance against various pathogens (Hu et al., 2017; Bacete et al., 2018), much remains to be learned about the molecular mechanisms they use to activate immune responses. The best-studied Wak protein, the Arabidopsis AtWAK1, recognizes cell-wall–derived oligogalacturonides (OGs) and activates OG-mediated defense responses against both fungal and bacterial pathogens (Brutus et al., 2010; Gramegna et al., 2016). In maize, the ZmWAK-RLK1 protein (encoded by *Htn1*) confers quantitative resistance to northern corn leaf blight by inhibiting the biosynthesis of secondary metabolites, benzoxazinoids, that suppress pathogen penetration into host tissues (Yang et al., 2019). Another ZmWAK protein encoded in a major head smut quantitative resistance locus *qHSR1* enhances maize resistance to *Sporisorium reilianum* by arresting the fungal pathogen in the mesocotyl (Zuo et al., 2015). One wheat Wak protein encoded by the *Stb6* gene recognizes an apoplastic effector (AvrStb6) from *Zymoseptoria tritici* and confers resistance to the fungal pathogen without a hypersensitive response (Saintenac et al., 2018). In rice, three OsWAKs act as positive regulators in resistance to the rice blast fungus by eliciting ROS production, activating defense gene expression, and recognizing chitin by being partially associated with the chitin receptor Chitin elicitor-binding protein (Delteil et al., 2016). Wak proteins therefore appear to exhibit extensive functional diversity and have different mechanisms to defend against pathogen infection in different plant species. The functional characterization of Wak proteins in tomato has not been reported and their possible contributions to PTI or NTI are not well understood in this species.

Tomato is an economically important vegetable crop throughout the world and its production is threatened by many pathogens including *Pst*, which causes bacterial speck disease and can result in severe crop losses (Jones, 1991; Kimura and Sinha, 2008). Understanding the functions of Wak proteins in tomato could therefore provide fundamental information for breeding tomato cultivars that are resistant to various pathogens. Tomato contains seven *Wak* and 16 *Wak-like kinase* genes (Zheng et al., 2016). The *SlWak1* (Solyc09g014720) gene is clustered together with another three *SlWak* genes (Solyc09g014710, Solyc09g014730, and Solyc09g014740) on chromosome 9; however, the expression of only the *SlWak1* gene (hereafter *Wak1*) is significantly induced after MAMP treatment or *Pst* inoculation (Rosli et al., 2013). Reduction of *Wak*1 gene expression in *N. benthamiana* leaves using virus-induced gene silencing (VIGS) compromised resistance to the bacterial pathogen *Pst*. However, three closely-related *NbWak* genes were simultaneously silenced in these experiments, making it unclear if one or a combination of *NbWak* genes contributed to the enhanced susceptibility to *Pst* (Rosli et al., 2013). To gain deeper insight into the role of *Wak1* in tomato-*Pst* interactions, we generated two homozygous *Wak1* mutant lines (Δwak1) in tomato using CRISPR/Cas9. Characterization of these Δwak1 mutants indicated that Wak1 protein acts as an important positive regulator in later stages of flagellin-mediated PTI response in the apoplast and associates in a complex with Fls2 and Fls3 to trigger immune signaling.

RESULTS

Generation of *Wak1* Mutants in Tomato by CRISPR/Cas9

We reported previously that VIGS of three homologs of *Wak1* in *N. benthamiana* led to enhanced susceptibility to *Pst* (Rosli et al., 2013). In tomato leaves, transcript abundance of the *Wak1* gene (Solyc09g014720) is significantly increased after treatment with flg22, flgII-28, or csp22, suggesting *Wak1* might play a role in tomato-*Pst* interactions (Rosli et al., 2013; Pombo et al., 2017). To study the possible role of *Wak1* in plant immunity, we generated mutations in *Wak1* using CRISPR/Cas9 with

a guide RNA (gRNA), Wak1-gRNA1 (GTTAAGATT AGCATAAAACA; Fig. 1A), which targets the first exon of the *Wak1* gene. After transformation of the cultivar Rio Grande-PtoR (RG-PtoR, which has the *Pto* and *Prf* genes), we obtained a biallelic mutant (Δwak1 4) from which two *Wak1* homozygous mutant lines (Δwak1 4-1; Δwak1 4-2) were derived (Fig. 1A). Line 4-1 has a 10-bp deletion in *Wak1*, resulting in a premature stop codon at the 17th amino acid of the protein, whereas line 4-2 has a 1-bp deletion in *Wak1*, causing a premature stop codon at the 18th amino acid (Fig. 1A). The growth, development, and overall morphology of both Δwak1 mutants were indistinguishable from wild-type RG-PtoR plants (Supplemental Fig. S1).

To determine if the gRNA designed for *Wak1* editing inadvertently caused mutations in other genomic regions of the Δwak1 plants, we selected seven putative sites with the highest off-target scores using Geneious R11 and Cas-OFFinder, although all of these sites had at least three mismatches compared with the spacer sequence of the *Wak1* gRNA (Fig. 1B). Of the seven potential off-target sites, two are located in the coding region of a gene, three are in the untranslated region of genes, and another two are in intergenic regions. For each site, we tested 10 to 20 independent T1 or T2 plants, with or without Cas9, and did not detect any off-target mutations. This is not unexpected, as the gRNA we designed for *Wak1* was highly specific, with little possibility to target *Wak1* homologs or other genes in tomato, considering that even one mismatch in the seed sequence (the last 12 nucleotides of a gRNA spacer sequence) can severely impair or completely abrogate the editing ability of the Cas9/gRNA complex (Jiang and Doudna, 2017).

Δwak1 Plants Are Compromised in PTI, But Not NTI, against *P. syringae* pv. Tomato

To test whether the response to *Pst* is affected in the Δwak1 plants, we vacuum-infiltrated Δwak1 and wild-type RG-PtoR plants with the *Pst* strain DC3000Δ*avrPto*Δ*avrPtoB* (DC3000ΔΔ), in which *avrPto* and *avrPtoB* have been deleted and therefore cannot activate NTI. Both Δwak1 lines showed enhanced disease symptoms compared to wild-type plants 4 d after bacterial inoculation, with ~6-fold more bacterial growth compared to the wild-type plants (Fig. 2A). No differences in symptoms or bacterial populations were observed between the Δwak1 and wild-type plants when they were inoculated with DC3000Δ*avrPto*Δ*avrPtoB*Δ*fliC* (DC3000ΔΔΔ; Fig. 2B), which lacks *avrPto* and *avrPtoB* and the flagellin-encoding gene *fliC*. This result indicates that Wak1 plays a role in flagellin-mediated PTI.

To test whether Wak1 contributes to NTI, the Δwak1, RG-PtoR, and Rio Grande-prf3 plants (RG-prf3, which contains a mutation in *Prf* that makes the Pto pathway nonfunctional) were inoculated with DC3000. Six days post inoculation (dpi), the Δwak1

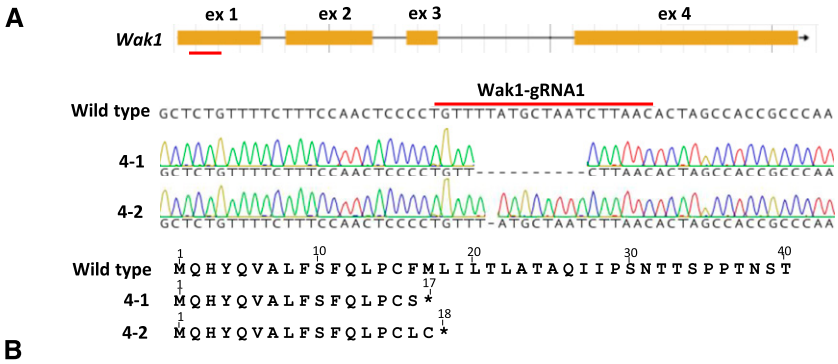

B

	Potential off-target*	Annotation of potential off-targets	No. of mismatches	Predicted by	No. of plants tested	No. of off-target mutations
1	GcTAgGATTAGCAgAAAACAAGG	Solyc08g079750 (exon 1)	3	Cas-OFFinder	20	0
2	GTTtAaATTAGCAgAAAACAAGG	Solyc07g063130 (3′ UTR)	3	Cas-OFFinder	20	0
3	GTcAAGATT-GCATcAAACATGG	Solyc02g081040 (5′ UTR)	3	Geneious	15	0
4	aTTgAGATTttCATAAAACAAGG	Solyc03g043720 (3′ UTR)	4	Geneious	15	0
5	aTTtAGAgTAGCATAAAAgAGGG	Solyc12g008360 (exon 8)	4	Geneious	15	0
6	GTTAgGATaAGCATAAAAaATGG	Intergenic	3	Cas-OFFinder & Geneious	10	0
7	GTTAAGATTgGtCATAAAACtGGG	intergenic	3	Cas-OFFinder	10	0

Figure 1. Generation of tomato *Wak1* mutants by CRISPR/Cas9. A, Schematics showing the gRNA target site in exon 1 (ex 1) and the missense mutations present in two Δwak1 lines (4-1 and 4-2). The gRNA was designed to target the first exon of the *Wak1* gene. The Δwak1 4-1 line has a 10-bp deletion and the Δwak1 4-2 line has a 1-bp deletion. Wild type is RG-PtoR. The Δwak1 lines have a premature stop codon at the 17th or 18th amino acid of the Wak1 protein. B, No mutations were detected in any of the potential off-target sites of the Δwak1 plants. For each potential off-target site, 10 to 20 individual plants (T1 or T2 plants) were tested. *PAM (NGG) is underlined; mismatching bases are shown in lowercase.

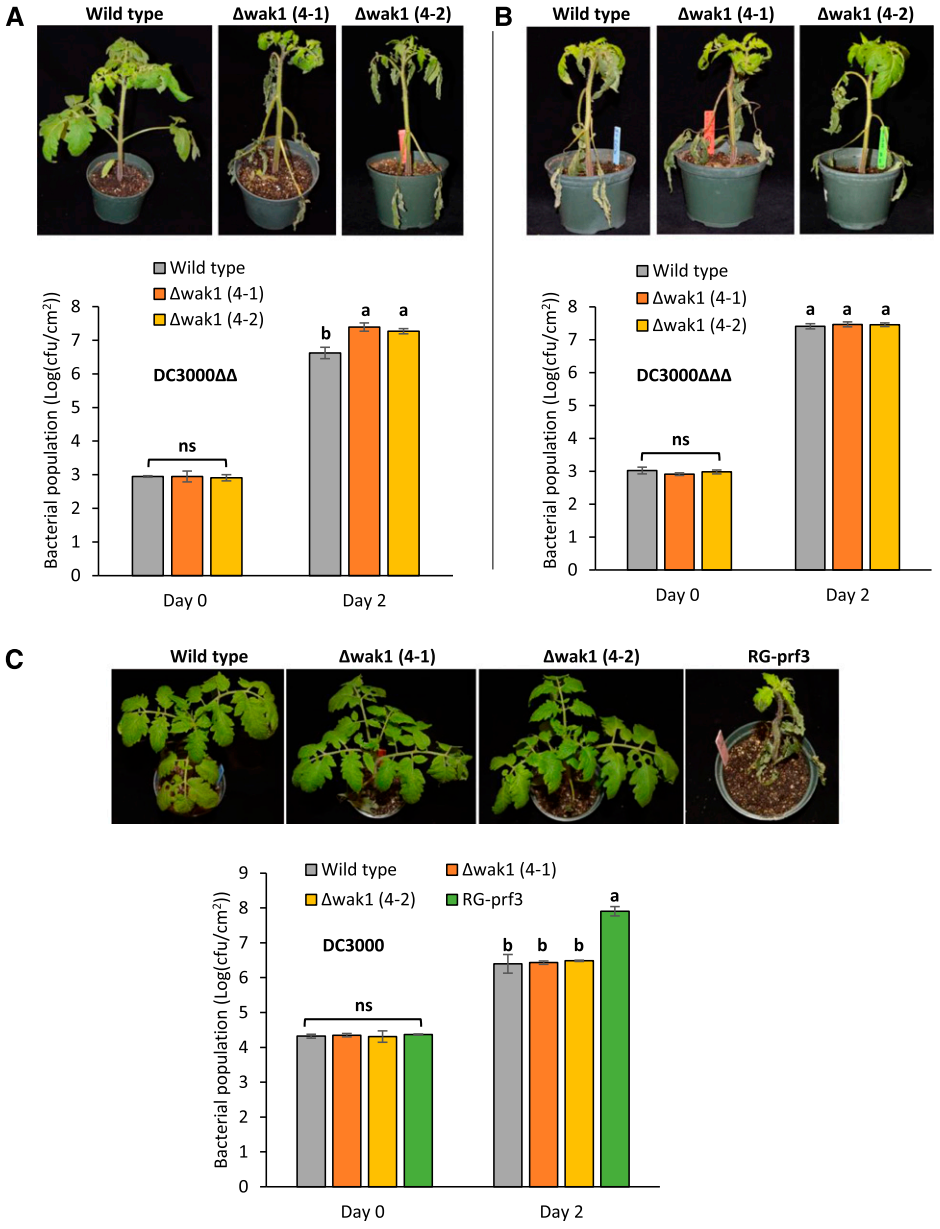

Figure 2. The Δwak1 tomato plants are compromised in flagellin-mediated PTI but unaffected in NTI. A to C, Four-week-old Δwak1 plants and wild-type RG-PtoR plants were vacuum-infiltrated with 5×10^4 cfu mL^{-1} DC3000Δ*avrPto*Δ*avrPtoB* (DC3000ΔΔ; A), 5×10^4 cfu mL^{-1} DC3000Δ*avrPto*Δ*avrPtoB*Δ*fliC* (DC3000ΔΔΔ; B), and 1×10^6 cfu mL^{-1} DC3000 (C). Photographs of disease symptoms were taken 4 (A and B) and 6 (C) dpi. Bacterial populations were measured at 3 h (day 0) and 2 d (day 2) after infiltration. Bars show means ± SD (SD). Different letters indicate significant differences based on a one-way ANOVA followed by Tukey's Honest Significant Difference post hoc test ($P < 0.05$). ns, No significant difference. Three or four plants for each genotype were tested per experiment. The experiment was performed three times with similar results.

and RG-PtoR plants had no disease symptoms, whereas the RG-prf3 control showed severe disease symptoms (Fig. 2C). Bacterial populations were ~30-fold less in the Δwak1 and RG-PtoR plants compared to RG-prf3. Wak1 therefore has no observable role in NTI.

The two Δwak1 mutant lines were derived from the same primary transformant and it was formally possible that another mutation induced during tissue culture is responsible for the enhanced susceptibility to *Pst*. We therefore developed F1 hybrids by crossing the Δwak1 plants to RG-PtoR plants (Supplemental Fig. S2). Sequencing confirmed that all F1 hybrids were heterozygous for the *Wak1* mutation. F1 hybrids that were vacuum-infiltrated with DC3000ΔΔ developed disease symptoms and supported bacterial populations similar to RG-PtoR plants (Supplemental Fig. S2A), indicating *Wak1* is a dominant allele. Four F1 plants (two were −10 bp/wild type and two were −1 bp/wild type) were selfed to develop F2 populations. After inoculation of 117 F2 plants with DC3000ΔΔ, we observed a segregation ratio of 3 (resistant) to 1 (susceptible; Supplemental Fig. S2B). Sequencing revealed all resistant plants were either homozygous wild type or heterozygous, while the susceptible plants were homozygous for the *wak1* mutation (Supplemental Fig. S2C). Combined with the lack of off-target mutations, these disease assays with F2 populations strongly support that the susceptibility to *Pst* of Δwak1 plants is due to the CRISPR/Cas9-induced loss-of-function mutations in the *Wak1* gene.

Wak1 Mutant Plants Are Compromised in PTI Induced by flg22 and flgII-28

The observation that Δwak1 plants are more susceptible to DC3000ΔΔ but show no differences compared to wild-type plants for their response to DC3000ΔΔΔ that lacks flagellin, suggests that Wak1 is involved in immune responses mediated by flg22 and/or flgII-28. To further test this, we performed a "PTI protection" assay using a heat-killed *Pst* strain lacking flagellin and three type-III effectors (DC3000Δ*avrPto*Δ*avrPtoB*Δ*hopQ1-1*Δ*fliC*; DC3000ΔΔΔΔ) complemented with a construct expressing *fliC* from either DC3000 (which has active flg22 and flgII-28) or *Pseudomonas cannabina* pv. alisalensis ES4326 (only flgII-28 is active; Hind et al., 2016), or an empty vector (EV) as a control (Fig. 3A). Because both of the Δwak1 lines were similarly susceptible to DC3000ΔΔ, most subsequent experiments were focused on the 4-1 line. Δwak1 4-1 plants were first infiltrated with the various suspensions of heat-killed bacteria to induce PTI and then challenged with DC3000ΔΔΔ 16 h later. Wild-type plants pretreated with *Pst* DC3000ΔΔΔΔ with an EV supported a significantly higher bacterial population than plants pretreated with the heat-killed bacterial suspensions containing either DC3000 *fliC* or ES4326 *fliC* (7.5-fold and 3.3-fold, respectively), indicating that pretreatment of wild-type plants activated PTI defenses due to recognition of flg22 and/or flgII-28. The Δwak1 plants, however, supported higher bacterial populations regardless of the pretreatment, indicating the PTI response was compromised (Fig. 3A).

We next performed the PTI protection assay using the synthetic peptides flg22 and flgII-28. Plants were first syringe-infiltrated with buffer alone, 1 μM of flg22, or 1 μM of flgII-28, and then challenged with DC3000ΔΔΔ 16 h later as described above (Fig. 3B). Two days later, wild-type plants that were pretreated with either flg22 or flgII-28 had significantly lower bacterial populations compared to the buffer-only treatment. In contrast, no significant differences in bacterial populations regardless of pretreatment were observed in Δwak1 plants. Collectively, these experiments demonstrate that Wak1 plays an important role in PTI that is activated by two flagellin-derived MAMPs.

Δwak1 Plants Are Not Compromised in PTI Responses on the Leaf Surface, or in Stomatal Numbers or Conductance

Pst inoculation experiments using vacuum infiltration assess PTI responses primarily in the apoplast. To test if Wak1-mediated immunity also plays a role in PTI on the leaf surface, we spray-inoculated Δwak1 and wild-type RG-PtoR plants with DC3000ΔΔ. This inoculation method requires the pathogen to enter the apoplastic space through stomata or natural openings. Interestingly, in contrast to experiments using vacuum infiltration, both wild-type and Δwak1 plants developed disease symptoms after spray inoculation that were indistinguishable both in the amount of time until they developed and in their ultimate severity (Fig. 4A). Consistent with this observation, there was no significant difference in DC3000ΔΔ populations in any of the lines after spray inoculation (Fig. 4B). Thus, Wak1 does not appear to play an important role in PTI responses on the leaf surface. Measurements of stomatal numbers and of stomatal conductance as an

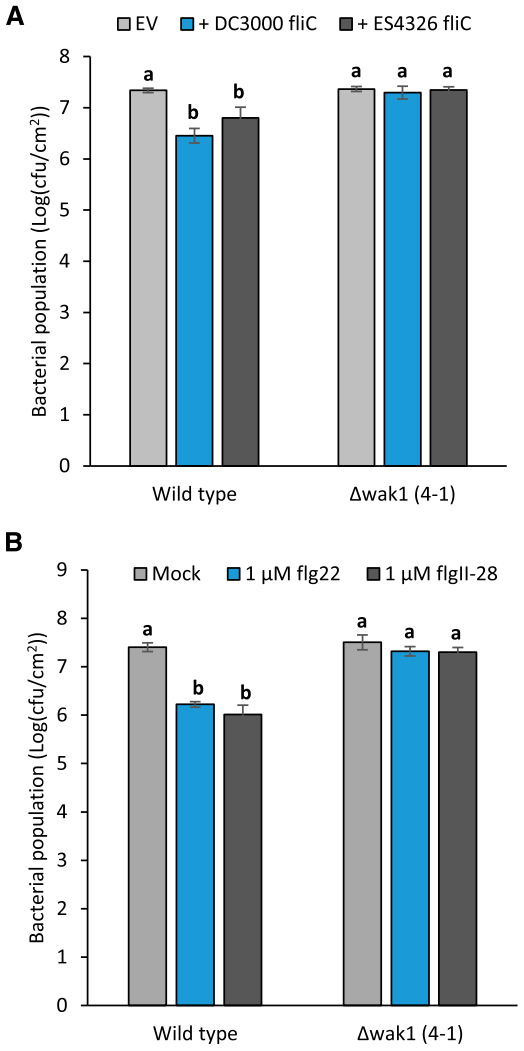

Figure 3. The Δwak1 plants are compromised in two PTI induction assays. A, Four-week-old Δwak1 plants (4-1) and wild-type RG-PtoR plants were first syringe-infiltrated with 1×10^8 cfu mL^{-1} of heat-killed DC3000Δ*avrPto*Δ*avrPtoB*Δ*hopQ1-1*Δ*fliC* (DC3000ΔΔΔΔ) complemented with a *fliC* gene from DC3000 or ES4326, or no *fliC* (EV). Sixteen hours later, the whole plants were vacuum-infiltrated with DC3000Δ*avrPto*Δ*avrPtoB*Δ*fliC* (DC3000ΔΔΔ) at 5×10^4 cfu mL^{-1}. Bacterial populations were measured 2 d after the infiltration. B, Plants (Δwak1 4-1 and wild type) were first syringe-infiltrated with buffer only (mock; 10 mM of $MgCl_2$), 1 μM of flg22, or 1 μM of flgII-28, respectively. Sixteen hours later, plants were vacuum-infiltrated with DC3000ΔΔΔ at 5×10^4 cfu mL^{-1}. Bacterial populations were measured 2 d later. Bars in A and B represent means ± SD. Different letters indicate significant differences based on a one-way ANOVA followed by Tukey's Honest Significant Difference post hoc test ($P < 0.05$).

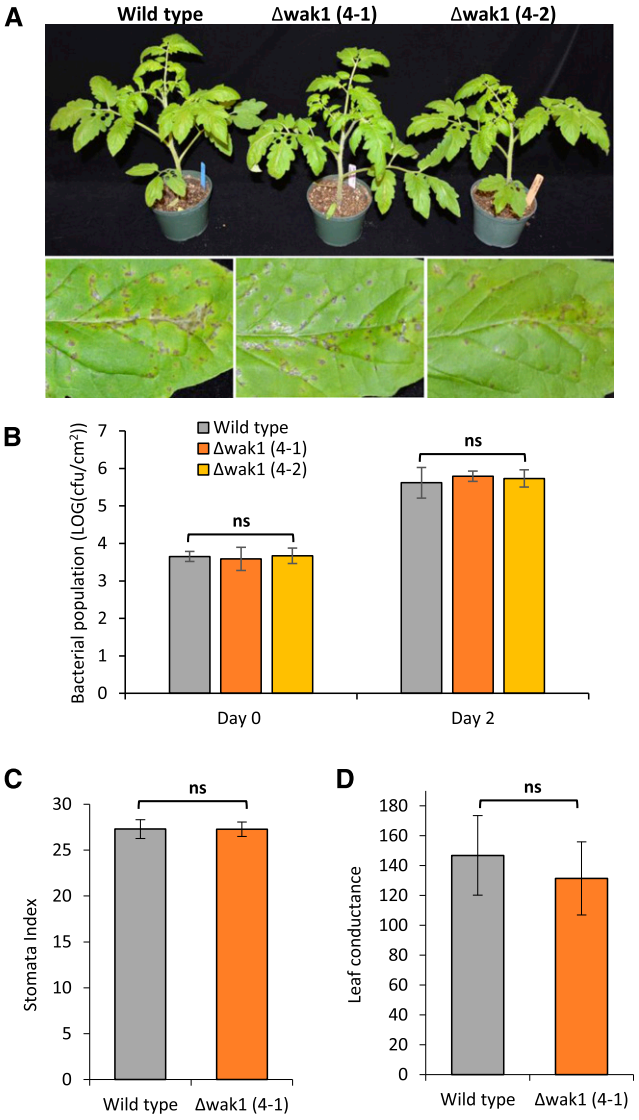

Figure 4. Leaf-surface–associated immune responses and stomata are unaffected in Δwak1 plants. A, Four-week-old Δwak1 plants and wild-type RG-PtoR plants were spray-inoculated with 1×10^8 cfu mL^{-1} DC3000Δ*avrPto*Δ*avrPtoB*. Photographs of disease symptoms were taken 6 dpi. Photographs show a representative plant and leaflet from each line. B, Bacterial populations were measured at 3 h (day 0) and 2 d (day 2) after spray inoculation. Bars show means ± SD. ns, No significant difference using a one-way ANOVA followed by Tukey's Honest Significant Difference post hoc test ($P < 0.05$). C, Stomatal index taken from wild-type and Δwak1 4-1 plants. Photographs from the abaxial epidermis of the leaves were taken using an epifluorescence microscope and the number of cells and both closed and open stomata were counted manually. The stomatal index was calculated as the percentage of stomata number per total number of cells (stomata plus epidermal cells). Five photographs per biological replicate were analyzed. Bars represent the mean of four biological replicates with their corresponding SD. D, Stomatal conductance (millimoles water) was measured on the abaxial side of leaflets on the third leaf. Data correspond to the average of two leaflets from at least four biological replicates per line, with ±SD. ns, No significant difference using Student's *t* test ($P < 0.05$).

indicator of stomatal activity revealed no differences between wild-type and Δwak1 plants, further indicating that Wak1 does not play a role at the leaf surface (Fig. 4, C and D).

Δwak1 Plants Are Unaffected in MAMP-Induced ROS Production or MAPK Activation, But Have Significantly Reduced Callose Deposition

Generation of ROS and activation of MAPK cascades are two typical early PTI-associated responses in plants (Nguyen et al., 2010; Zipfel, 2014). To investigate whether Wak1 participates in these responses, we first performed ROS assays using flg22, flgII-28, or csp22. We observed no differences in ROS production in Δwak1 plants compared to wild-type plants when treated with any of these MAMPs (Fig. 5, A and B; Supplemental Figs. S3 and S4). We also observed no difference between wild-type and Δwak1 plants for their ability to activate MAPKs in response to flg22 and flgII-28 (Fig. 5C).

Callose deposition is a response associated with later stages of PTI, and one that is regulated independently or downstream of MAPK activation (Li et al., 2016). We measured callose deposition by challenging Δwak1 and wild-type plants using a nonpathogenic bacterial strain, *Pseudomonas fluorescens* 55, a strong inducer of PTI (Rosli et al., 2013). Compared to wild-type plants, Δwak1 plants showed significantly reduced callose deposition 1 d after vacuum infiltration of *Pf* 55 (Fig. 5D). These observations therefore indicate that Wak1 functions at a later stage of the PTI response in a flagellin-induced process independent of ROS production and MAPK activation.

The Increase in *Wak1* Transcript Abundance upon flgII-28 Treatment Is Fls3-Dependent

In tomato, the transcript abundance of *Wak1* is low in unchallenged conditions, but is significantly higher after *Pst* inoculation (Rosli et al., 2013). To gain insight into the transcriptional regulation of *Wak1* and *Fls3* during the immune response, we used reverse-transcription quantitative PCR (RT-qPCR) to measure *Wak1* and *Fls3* transcript abundance after treatment of wild-type leaves with flgII-28 (Fig. 6A). The relative abundance of *Wak1* or *Fls3* transcripts at various time points after syringe-infiltrating 1 μM of flgII-28 was compared to a mock treatment (10 mM of $MgCl_2$). Both *Wak1* and *Fls3* transcript abundance increased significantly at 6 and 8 h after syringe-infiltrating flgII-28 compared to the mock control (Fig. 6A).

To investigate possible codependence of *Wak1* and *Fls3* gene expression, we measured the *Wak1* transcript abundance in tomato plants that have mutations in the two *Fls2* genes and *Fls3* (Δfls2.1/2.2/3; R. Roberts, A.E. Liu, L. Wan, A.M. Geiger, and G.B. Martin,

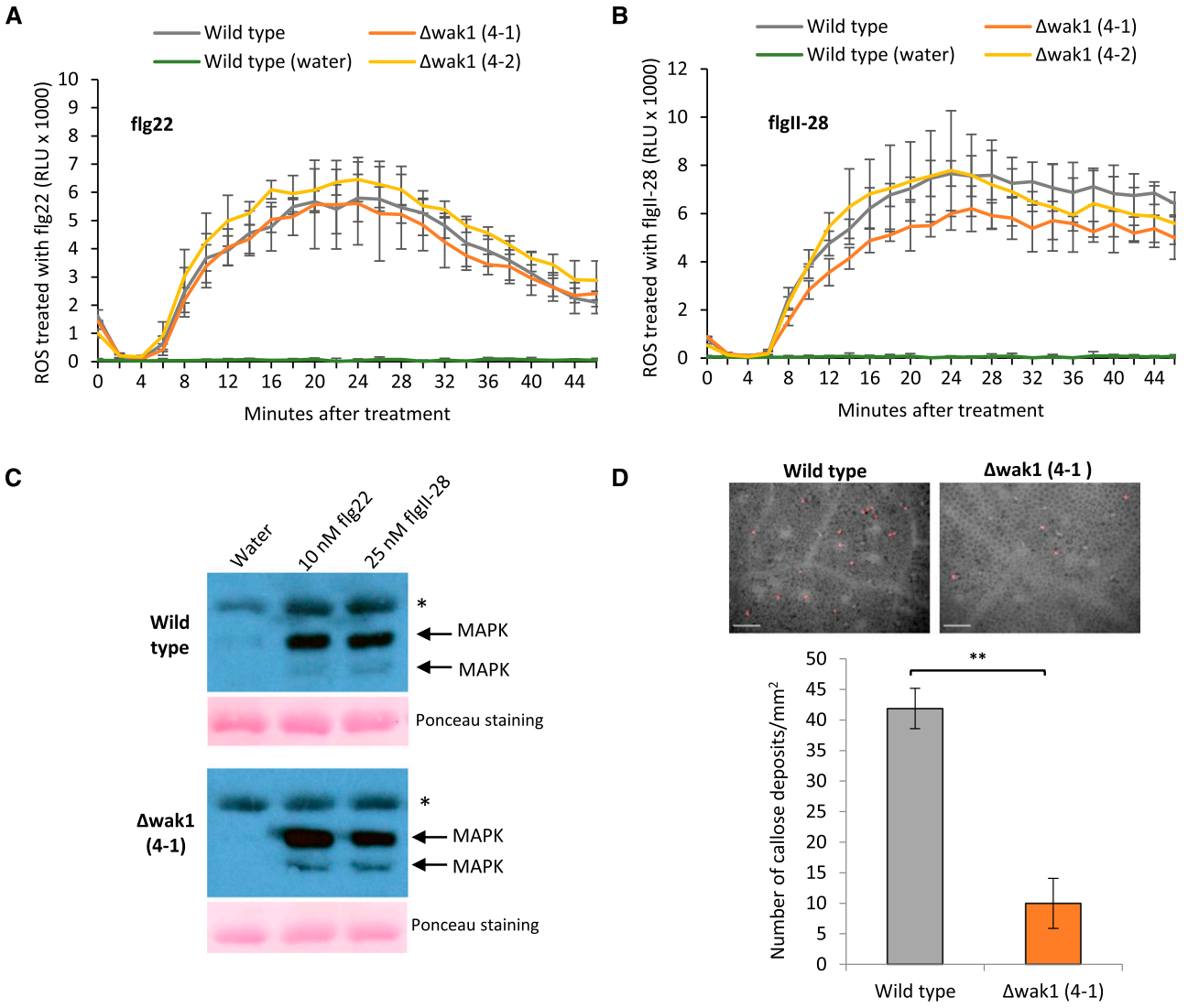

Figure 5. The Δwak1 plants are not affected in MAMP-induced ROS production or MAPK activation but have reduced callose deposition. Leaf discs from Δwak1 or wild-type plants were treated with 50 nM of flg22 (A), 50 nM of flgII-28 (B), or water only, and relative light units (RLUs) were measured over 45 min. One-way ANOVA followed by Tukey's Honest Significant Difference post hoc test ($P < 0.05$) was performed at 24 min (peak readout) and 45 min after treatment with flg22 or flgII-28. No significant difference was observed between Δwak1 and wild-type plants in either treatment. C, Leaf discs from Δwak1 (4-1) or wild-type RG-PtoR plants were treated with water, 10 nM of flg22, or 25 nM of flgII-28 for 10 min. Proteins were extracted from a pool of discs from three plants and subjected to immunoblotting using an antipMAPK antibody that detects phosphorylated MAPKs. The photographs shown are derived from the same immunoblot with identical exposure times. Ponceau staining and the nonspecific band (*) indicate equal loading of protein. This experiment was performed three times with similar results. D, Wild-type and Δwak1 plants (4-1) were vacuum-infiltrated with 1×10^8 cfu mL^{-1} *P. fluorescens* 55. Leaf samples were taken 24 h after infiltration, de-stained with 96% ethanol, and stained with aniline blue for 1 h. Callose deposits were analyzed using an epifluorescence microscope. Top, Representative photographs of wild-type and Δwak1 plants taken for callose deposition estimation. Red spots indicate the callose deposits observed and used for quantification. Scale bars = 100 μm. Bottom, Total number of callose deposits per mm^2 quantified in each group of plants. Fifteen photographs per biological replicate were analyzed. Bars represent the mean of four biological replicates with their corresponding SD. The asterisks represent a significant difference using Student's *t* test (**$P < 0.01$).

unpublished data) and the *Fls3* transcript abundance in Δwak1 plants after treatment with flgII-28. The abundance of *Wak1* transcripts was greatly reduced in the Δfls2.1/2.2/3 plants compared to wild-type plants, whereas *Fls3* abundance was not significantly different in Δwak1 or wild-type plants (Fig. 6, B and C). These results indicate that *Wak1* gene expression is regulated by the Fls3 pathway and its function likely occurs downstream of the mechanism inducing *Fls3* gene expression.

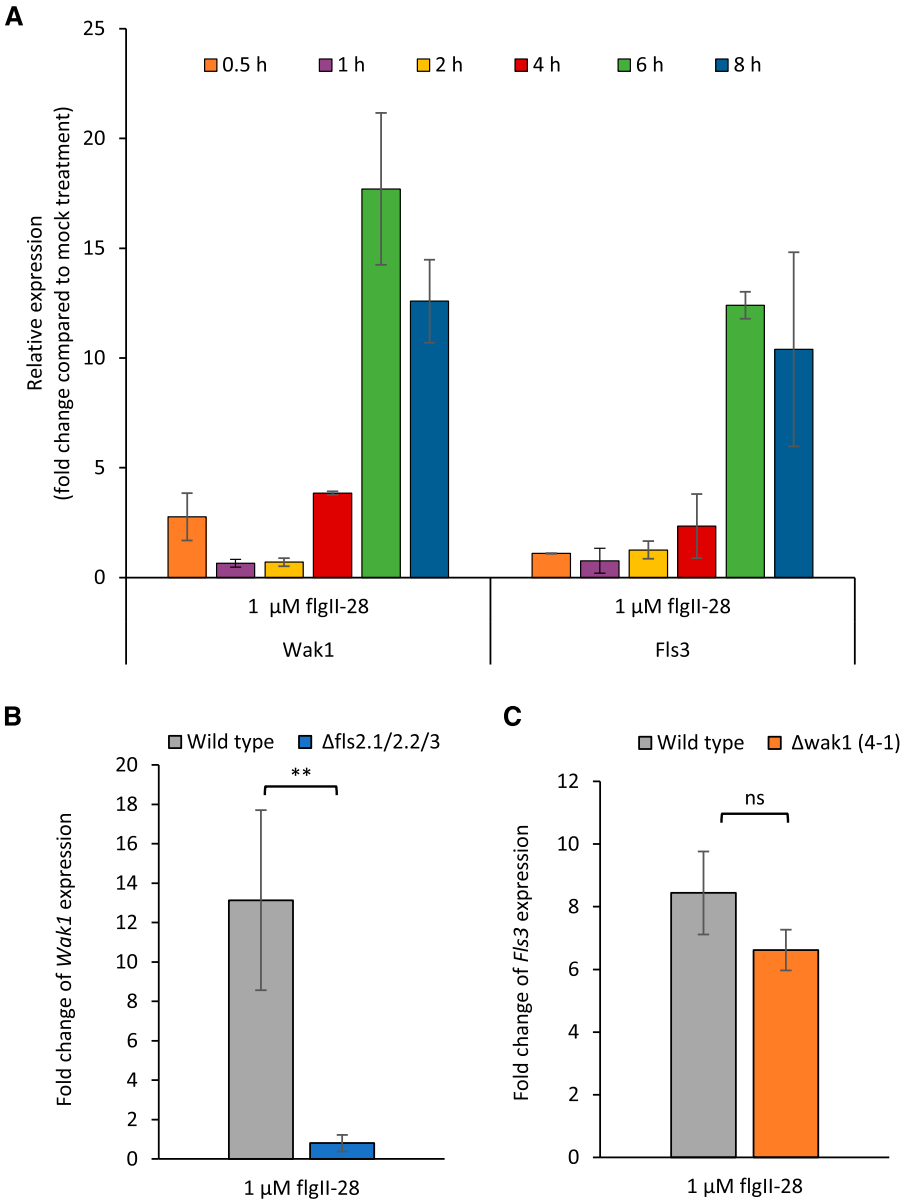

Figure 6. Transcript abundance changes of *Wak1* are dependent on the presence of Fls3 in tomato. A, Transcript abundance of *Wak1* and *Fls3* genes measured by RT-qPCR at the times shown after treatment with 1 μM of flgII-28 compared to a buffer-only control (10 mM of $MgCl_2$; mock treatment). Each treatment included three biological replicates and three technical replicates. *SlArd2* (Solyc01g104170) was used as the reference gene for quantification. Bars represent means ± SD. B, RT-qPCR was used to measure transcript abundance of *Wak1* 6 h after treatment of Δfls2.1/2.2/3 or wild-type leaves with 1 μM of flgII-28. Bars represent the mean ± SD. Asterisks indicate a significant difference using Student's *t* test (**$P < 0.01$). C, RT-qPCR was used to measure transcript abundance of *Fls3* 6 h after treatment of Δwak1 (4-1) or wild-type leaves with 1 μM of flgII-28. Bars represent the mean ± SD. ns, No significant difference using Student's *t* test ($P < 0.05$).

Δwak1 Plants Develop Bacterial Speck Disease Symptoms More Slowly than Δfls2.1/2.2/3 Plants

To determine the relative contributions of Wak1 and Fls2/Fls3 to PTI, we next compared the response of Δwak1 and Δfls2.1/2.2/3 plants to DC3000ΔΔ (Fig. 7). Three days after inoculation, the Δfls2.1/2.2/3 plants showed more severe disease symptoms than Δwak1 plants or wild-type plants, but by 4 dpi both the Δwak1 and Δfls2.1/2.2/3 plants developed more disease symptoms than the wild-type plants (Fig. 7A). There was no visible difference in disease symptoms between the Δwak1 and Δfls2.1/2.2/3 plants 4 to 10 dpi (Fig. 7A). Two days after inoculation, the bacterial population in the Δfls2.1/2.2/3 and Δwak1 plants was 6-fold and 4-fold higher than the wild-type plants, respectively, with no statistically significant difference in bacterial populations between the Δwak1 and Δfls2.1/2.2/3 plants (Fig. 7B). Thus, although there was a delay in disease progression at the whole plant level, this delay was not reflected in a difference in bacterial populations at 2 dpi. A delay in disease progression would be expected if the *fls2.1/2.2/3* mutations result in the loss of both early and later-stage PTI whereas the *wak1* mutation compromises primarily later-stage PTI responses.

Wak1 Occurs in a Complex with Fls2 and Fls3 Independent of flg22, flgII-28, or BAK1

The results above indicate that Wak1 plays a major role in flg22- and flgII-28-induced processes that occur in the apoplast later in the PTI response. We considered

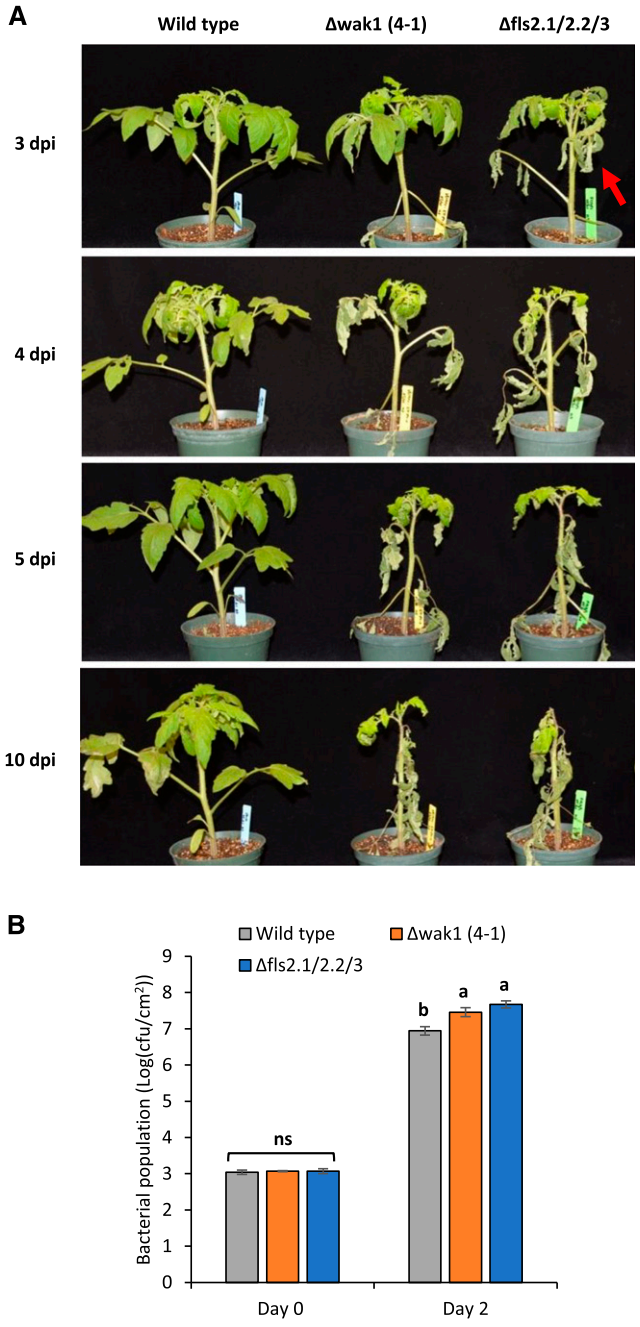

Figure 7. The Δwak1 plants develop disease symptoms more slowly than Δfls2.1/2.2/3 plants. Four-week-old Δwak1 (4-1), Δfls2.1/2.2/3 or wild-type RG-PtoR plants were vacuum-infiltrated with 5×10^4 cfu mL^{-1} DC3000Δ*avrPto*Δ*avrPtoB*. A, Photographs were taken at 3, 4, 5, or 10 dpi. The red arrow points to more extensive disease on the Δfls2.1/2.2/3 plant at 3 dpi. B, Bacterial populations were measured 3 h (day 0) and 2 dpi (day 2). Bars represent means ± SD. Different letters indicate significant differences based on a one-way ANOVA followed by Tukey's Honest Significant Difference post hoc test ($P < 0.05$). ns, No significant difference. Three or four plants for each genotype were tested per experiment. This experiment was performed twice with similar results.

the possibility that Wak1 acts in a complex with Fls2 and Fls3 similar to what has been reported for FLS2 and FERONIA (FER) in Arabidopsis (Stegmann et al., 2017). We therefore used transient expression of proteins in *N. benthamiana* leaves and coimmunoprecipitation to investigate if Wak1 physically associates with Fls2, Fls3, or the coreceptor BAK1 and, if so, whether the interaction is affected by the presence of flg22 or flgII-28. We observed a weak, but reproducible and specific, interaction of Wak1 with both Fls2 and Fls3 with the interactions occurring independently of flg22, flgII-28, or the presence of BAK1(Fig. 8A; Supplemental Fig. S5). As expected, Fls3 and Fls2 each interacted strongly with BAK1 only in the presence of flgII-28 or flg22, respectively. No interaction was observed between Wak1 and BAK1 proteins (Fig. 8B). Additionally, Wak1 did not affect the accumulation of the Fls2, Fls3, or BAK1 proteins or vice versa (Fig. 8; Supplemental Fig. S5).

DISCUSSION

The tomato *Wak1* gene was first identified as a flagellin-induced, repressed-by-effectors gene in the immune response against *P. syringae* (Rosli et al., 2013). When its expression was reduced by VIGS in *N. benthamiana*, the morphology of the plants was unaffected but their ability to activate PTI was compromised, leading to more severe disease symptoms and enhanced growth of a virulent *Pst* strain (Rosli et al., 2013). The interpretation of these experiments was limited somewhat by the fact that three *N. benthamiana Wak1* homologs were silenced by the tomato *Wak1* VIGS construct and, as is typical for VIGS, their transcripts were not completely eliminated (they were reduced by ~50%). Thus, whether one, or more, of the *Wak1* homologs in *N. benthamiana* play a role in PTI was unclear as was the degree to which a complete knockout of the *Wak1* genes might affect PTI or affect plant morphology. Here we have addressed these limitations by developing two CRISPR/Cas9-mediated *Wak1* mutants in tomato and using them to investigate the contributions of Wak1 to several PTI-associated responses and to resistance to *P. syringae*. As elaborated upon below, our results indicate *Wak1* gene expression is induced by the Fls2 and Fls3 pathways in tomato; the Wak1 protein associates in a complex with Fls2 and Fls3; and Wak1 plays an important role in later stages of flagellin-induced PTI.

Consistent with our earlier observations of *Wak1*-silenced *N. benthamiana* plants, the Δwak1 tomato plants developed more severe disease symptoms compared to wild-type plants and supported larger populations of *Pst*; they also had wild-type morphology. Interestingly, the differences in pathogen responses were abolished when the *Pst* strain used for inoculation lacked flagellin, suggesting that either flg22 and/or flgII-28 and their corresponding receptors Fls2 and Fls3 play a key role in activating Wak1-mediated responses. In fact, subsequent experiments using *Pst* strains with

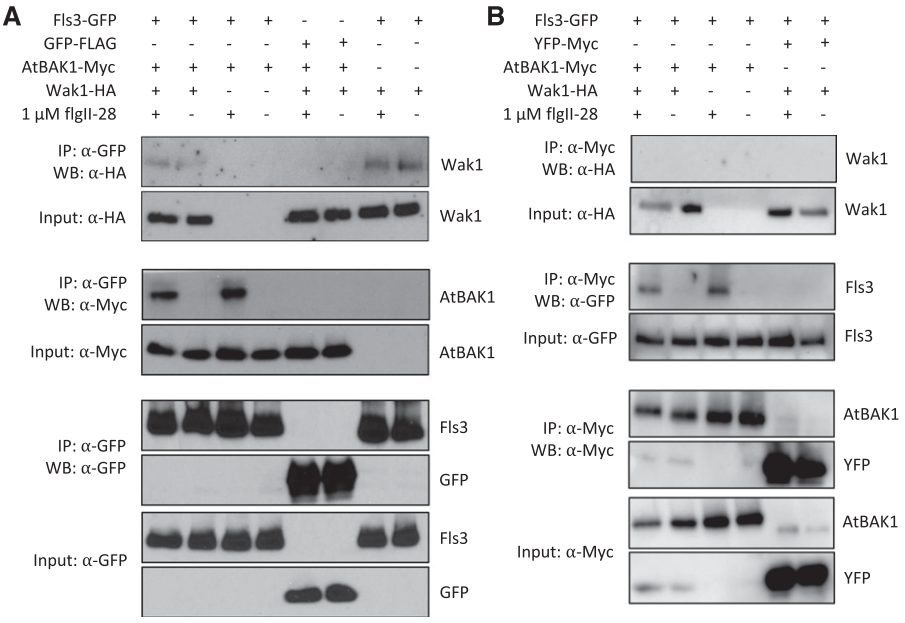

Figure 8. Wak1 associates with Fls3 independently of flgII-28 and BAK1, and Wak1 does not associate with BAK1. Proteins were extracted from *N. benthamiana* leaves expressing Fls3-GFP in combination with AtBAK1-Myc and/or Wak1-HA after treatment with or without 1 μM of flgII-28 for 2 min and were used for immunoprecipitation using anti-GFP magnetic agarose beads (A) or anti-Myc magnetic beads (B). Wak1 was pulled down with Fls3 (A) but not with BAK1 (B) after treatment with or without flgII-28. Wak1, BAK1, Fls3, GFP, and Yellow Fluorescent Proteins (YFP) were detected by immunoblotting with α-HA, α-Myc, or α-GFP antibodies. This experiment was repeated three times with similar results.

variant FliC proteins, or using synthetic flg22 and flgII-28 peptides, confirmed that either one of these MAMPs is sufficient to induce Wak1-dependent PTI. At this stage of the work this dependence potentially could be explained simply by the fact that both of these MAMPs are able to significantly upregulate expression of the *Wak1* gene.

Several observations support the hypothesis that Wak1 acts at a later stage of the PTI response in tomato. First, the Δwak1 plants showed no difference from wild-type plants when *Pst* was spray-inoculated, a method that assays for PTI responses at the leaf surface. The importance of PTI on the leaf surface has been extensively documented in Arabidopsis where a major regulator of this response is the activity of FLS2 in the stomata (Melotto et al., 2006, 2008, 2017). Our observations suggest that Wak1 does not act in PTI on the leaf surface but instead exerts its function at a later stage, after *Pst* enters the apoplastic space as simulated by vacuum infiltration. Second, Δwak1 plants showed no defects in their ability to produce ROS upon exposure to csp22, flg22, or flgII-28 or activate MAPKs in response to flg22 and flgII-28. Both of these responses occur early (within minutes) in leaves that are exposed to MAMPs. Third, *Fls3* gene expression induced by flgII-28 was the same in Δwak1 plants as it was in wild-type plants. Transcriptional changes also occur rapidly (within 1 h) of MAMP treatment (Pombo et al., 2017). As expected, the induction of *Wak1* gene expression by flgII-28 was compromised in Δfls2.1/2.2/3 plants. Fourth, the Δwak1 plants produced just 25% of the callose deposits observed in wild-type plants in response to *P. fluorescens*, a source of flagellin and other MAMPs. Callose deposition occurs later than ROS production and MAPK activation, and contributes to cell-wall strengthening that may inhibit the infection process (Nguyen et al., 2010; Voigt, 2014). Finally, the Δwak1 plants developed disease symptoms more slowly than did Δfls2.1/2.2/3 plants. This would be expected if the Δfls2.1/2.2/3 mutations result in the loss of both early (e.g. ROS, MAPK activation, transcriptional reprogramming) and later-stage PTI (callose deposition), whereas the *Wak1* mutation compromises primarily later-stage PTI responses. Importantly, however, both Δwak1 and Δfls2.1/2.2/3 plants ultimately developed the same severe disease symptoms that demonstrate the critical role that Wak1 plays in the host response to *Pst*.

The dependence of Wak1-mediated PTI on Fls2 and Fls3 activity could be explained, in part, by the induction of *Wak1* gene expression by the Fls2 and Fls3 pathways. However, our observations also raised the possibility that Wak1 resides in a complex that contains Fls2 and Fls3 and its function involves these receptors. We tested this hypothesis and found that Wak1 does coimmunoprecipitate with Fls2 and Fls3 in a MAMP-independent manner and it does not affect accumulation of Fls2/Fls3 proteins. This is reminiscent of the Arabidopsis malectin-like receptor kinase, FER, which was found to weakly associate with FLS2 independent of flg22 treatment and also had no effect on FLS2 accumulation (Stegmann et al., 2017). It is possible that Wak1, like FER, may act as an important cell-wall–associated scaffold to regulate immune receptor-complex formation. Tomato Wak1 did not coimmunoprecipitate with BAK1, and BAK1 was not required for the Wak1-Fls2/Fls3 interactions. In contrast, FER weakly associates with BAK1 and the interaction is enhanced upon flg22 treatment, but whether BAK1 is required for the weak association of FER-FLS2 was not investigated (Stegmann et al., 2017).

Based on our observations, we propose a model for the role of Wak1 in PTI (Fig. 9). In this model, *Wak1* transcript abundance is greatly increased upon

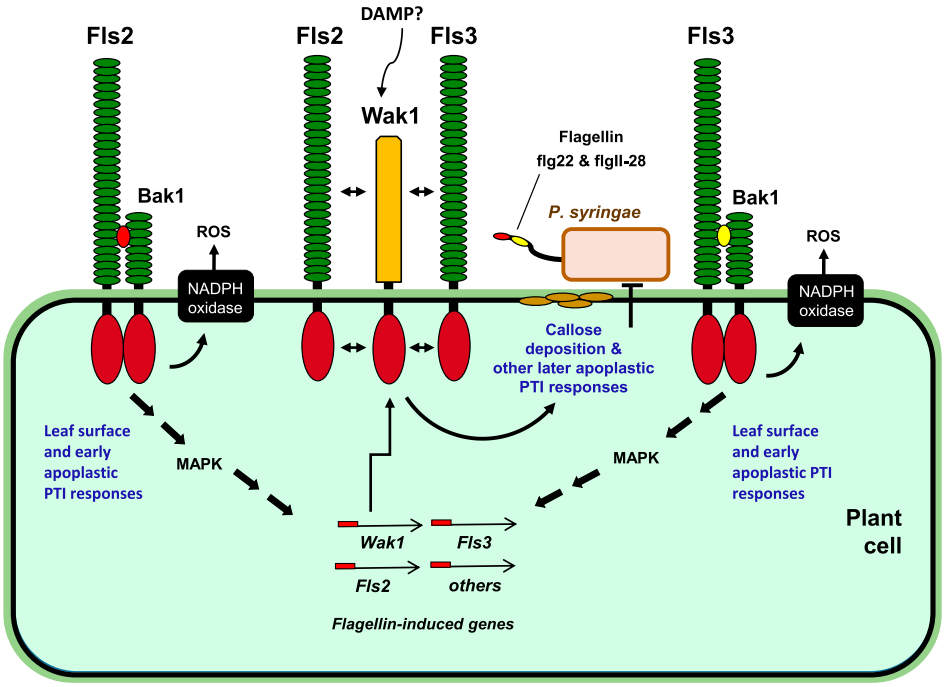

Figure 9. A model for the role of SlWak1 in PTI. Transcript abundance of *Wak1* increases in mesophyll cells upon activation of the Fls2 or Fls3 pathways. This leads to increased accumulation of Wak1 protein, which is then localized to the cell wall and here it joins a complex containing Fls2 and Fls3. Wak1 might act as a scaffold and could be a receptor for a DAMP. Wak1 functions to promote deposition of callose at the cell wall and other immune responses that inhibit multiplication of the pathogen.

activation of the PRRs Fls2 and Fls3. We hypothesize this gene expression occurs primarily when *Pst* enters the apoplastic space and that *Wak1* is not expressed in leaf surface or stomatal cells. Increased transcript abundance leads to increased Wak1 protein accumulation and subsequent localization to a cell-wall–associated protein complex that contains Fls2 and Fls3 and possibly other PRRs. Wak1 might act as a receptor of a damage-associated molecular pattern (DAMP), such as OGs. Binding of such a DAMP might impact the association of Wak1 with the Fls2/Fls3 complex to promote stabilization and accumulation of the PRRs, enhance the interaction of Wak1 with PRRs, or possibly stimulate PRR kinase activity. Whatever the mechanism, the presence of Wak1 in this Wak plays a critical role in later stages of PTI, including callose deposition and other processes that ultimately inhibit growth of virulent *Pst*.

This model gives rise to several questions that will need to be addressed in the future. First, why is Wak1 not active in plant cells on the leaf surface, including stomata, but only functions when *Pst* enters the apoplastic space? This could be due to lack of *Wak1* gene expression, protein accumulation, association with the Fls2/Fls3 complex, or kinase activity in leaf surface cells. Second, how does Wak1 affect the cell-wall–associated Fls2/Fls3 complex and is its activity in this complex influenced by perception of a DAMP? In Arabidopsis, AtWAK1 was demonstrated to bind pectin and OGs in vitro (Kohorn et al., 2009), and was identified as the receptor for OGs in vivo (Brutus et al., 2010). Does Wak1 bind OGs and, if so, do OGs impact the way Wak1 associates with Fls2/Fls3 and its role in PTI? Finally, it will be interesting to investigate possible differences in the transcriptome, metabolome, and proteome of the Δwak1 mutants in comparison with wild-type plants to understand what are the later PTI responses to which Wak1 contributes.

CONCLUSION

We generated two *SlWak1* tomato mutants (Δwak1s) using CRISPR/Cas9 and investigated the role of *SlWak1* using various *Pst* strains, immune response assays, RT-qPCR, and protein biochemistry. We discovered that late PTI responses activated by flg22 or flgII-28 are compromised in the apoplast but not on the leaf surface in Δwak1 plants. Δwak1 plants developed fewer callose deposits than wild-type plants but retained the ability to activate early PTI responses such as generation of ROS and activation of MAPKs upon exposure to flg22 and flgII-28. After *Pst* inoculation, Δwak1 plants developed disease symptoms more slowly than Δfls2.1/2.2/3 mutant plants, although both plants ultimately were similarly susceptible. SlWak1 coimmunoprecipitated with both Fls2 and Fls3 independently of flg22/flgII-28 or BAK1. These observations suggest that SlWak1 acts in a complex with Fls2/Fls3, and plays an important role at later stages of the PTI in the apoplast.

MATERIALS AND METHODS

Generation of *Wak1* Tomato Mutants Using CRISPR/Cas9

To mutate the *Wak1* gene in tomato (*Solanum lycopersicum*), we designed two gRNAs (Wak1-gRNA1: GTTAAGATTAGCATAAAACA and Wak1-gRNA2: GGGGCGGTGGCATTCGTTGG; Supplemental Table S1) targeting the first exon of *Wak1* using the software Geneious R11 (Kearse et al., 2012). Each gRNA

cassette was cloned into a Cas9-expressing binary vector (p201N:Cas9) by Gibson assembly as described in Jacobs et al. (2017). Tomato transformation was performed at the biotechnology facility at the Boyce Thompson Institute. *Agrobacterium* cells containing each gRNA/Cas9 construct were pooled together and used for transformation into the tomato cultivar RG-PtoR, which has the *Pto* and *Prf* genes. To determine the mutation type, genomic DNA was extracted from cotyledons or young leaves of each transgenic plant using a modified cetyl trimethylammonium bromide method (Murray and Thompson, 1980). Genomic regions spanning the target site of the *Wak1* gene were amplified with specific primers (Supplemental Table S1) and sequenced at the Biotechnology Resource Center at Cornell University. Geneious R11 and the web-based tool called Tracking of Indels by Decomposition (https://tide.deskgen.com; Brinkman et al., 2014) were used to determine the mutation type and frequency using the sequencing files (ab1. format) as described in Zhang et al. (2020).

Off-Target Evaluation

To investigate potential off-target mutations caused by gRNAs in the Δwak1 plants, Wak1-gRNA1, which induced target mutations in *Wak1* in the transgenic plants, was used as a query to search putative off-target sites across the tomato genome with up to four nucleotide mismatches by Geneious R11 or with up to three nucleotide mismatches by Cas-OFFinder (Bae et al., 2014). Seven potential off-target sites with the highest similarity to the spacer sequence of Wak1-gRNA1 were chosen for evaluation. Genomic regions spanning the putative off-target sites were amplified with specific primers (Supplemental Table S1) and PCR amplicons were sequenced to determine if off-target mutations were induced at those sites.

Bacterial Inoculation Assay

Four-week–old Δwak1 and wild-type plants were vacuum-infiltrated with various *Pst* DC3000 strains at different titers, including DC3000Δ*avrPto*Δ*avrPtoB* (DC3000ΔΔ) or DC3000Δ*avrPto*Δ*avrPtoB*Δ*fliC* (DC3000ΔΔΔ) at 5×10^4 cfu mL^{-1} or DC3000 at 1×10^6 cfu mL^{-1}. Three to four plants per line were tested with each bacterial strain. Bacterial populations were measured at 3 h and 2 dpi. Disease symptoms were photographed 4 or 5 d after bacterial infection. Δwak1 and wild-type plants were also spray-inoculated with DC3000ΔΔ at 1×10^8 cfu mL^{-1}. In this case, the leaf surfaces were sterilized with 15% H_2O_2 for 5 min and then rinsed thoroughly with sterile water before sampling for measuring bacterial populations. Photographs of disease symptoms were taken at 6 dpi.

PTI Protection Assay

Four leaflets on the third leaf of 4-week-old plants were first syringe-infiltrated with 1×10^8 cfu mL^{-1} of heat-killed DC3000Δ*avrPto*Δ*avrPtoB*Δ*hopQ1-1*Δ*fliC* (DC3000ΔΔΔΔ) complemented with a *fliC* allele from DC3000 or ES4326, or no *fliC* (EV). Note that *hopQ1* was deleted from this strain to allow its use on *Nicotiana benthamiana* where HopQ1 activates NTI, but HopQ1 is not relevant to the experiment shown in Figure 3A. Sixteen hours later, whole plants were vacuum-inoculated with DC3000Δ*avrPto*Δ*avrPtoB*Δ*fliC* (DC3000ΔΔΔ) at 5×10^4 cfu mL^{-1}. Bacterial populations were measured at 2 dpi. Alternatively, plants were first syringe-infiltrated with 1 μM of flg22 (GenScript), 1 μM of flgII-28 (EZBiolab), or buffer alone (10 mM of $MgCl_2$), respectively. Plants were inoculated with DC3000ΔΔΔ 16 h later and bacterial populations were measured at 2 dpi as described above.

Measurement of Stomata Number and Stomata Conductance

Leaf samples were taken from Δwak1 and wild-type plants. Photographs from the abaxial epidermis of the leaves were taken using a model no. BX51 epifluorescence microscope (Olympus) and the number of cells and both closed and open stomata were counted manually. The stomata index was calculated as the percentage of stomata number per total number of cells (stomata plus epidermal cells). Stomatal conductance was measured at 2 PM (8 h after lights went on), using a leaf porometer (SC1 Decagon Devices) on the abaxial side of two leaflets of the third leaf from four plants per line.

ROS Assay

ROS production was measured as described in Hind et al. (2016). In brief, leaf discs were collected and floated in water overnight (~16 h). Water was then removed and replaced with a solution containing either 50 nM of flg22 (QRLSTGSRINSAKDDAAGLQIA) or 50 nM of flgII-28 (ESTNILQRMRELAVQSRNDSNSSTDRDA), in combination with 34 μg mL^{-1} of luminol (Sigma-Aldrich) and 20 μg mL^{-1} of horseradish peroxidase. ROS production was then measured over 45 min using a Synergy-2 microplate reader (BioTek). Three to four plants per line and three discs per plant were collected for each experiment.

MAPK Phosphorylation Assay

Six leaf discs of Δwak1 and wild-type plants were floated in water overnight to let the wound response subside. The leaf discs were then incubated in 10 nM of flg22, 25 nM of flgII-28, or water (negative control) for 10 min, and immediately frozen in liquid nitrogen. Protein was extracted using a buffer containing 50 mM of Tris-HCl at pH 7.5, 10% (v/v) glycerol, 2 mM of EDTA, 1% (v/v) Triton X-100, 5 mM of ditiothreitol, 1% (v/v) protease inhibitor cocktail (Sigma-Aldrich), and 0.5% (v/v) Phosphatase inhibitor cocktail 2 (Sigma-Aldrich). MAPK phosphorylation was determined using an antiphospho-p44/42 MAPK (Erk1/2) antibody (antipMAPK; Cell Signaling).

Callose Deposition

Four-week–old plants were vacuum-infiltrated with 1×10^8 cfu mL^{-1} *Pseudomonas fluorescens* 55, a strong inducer of PTI (Rosli et al., 2013). Leaf samples were taken 24-h post infiltration, cleared with 96% ethanol, and stained with aniline blue for 1 h. Callose deposits were visualized with an epifluorescence microscope (BX51; Olympus). For each of the images analyzed, callose deposits were first selected manually to avoid counting trichomes or stomata. Valid deposits consisted of spots ranging between 57 and 5,674 μm^2 (8.5–85-μm diameter) as described in Nguyen et al. (2010). Quantification was performed using the Fiji package in the software ImageJ (https://imagej.nih.gov/ij/). Fifteen photographs per biological replicate were analyzed using four plants per line.

Coimmunoprecipitation

Agrobacterium tumefaciens strains (GV3101+ pMP90) carrying a Gateway binary vector with *Fls2*, *Fls3*, *BAK1*, *Wak1*, or *GFP/YFP)* were infiltrated into leaves of 4-week-old *N. benthamiana*. Leaves were treated with either 1 μM of flg22, 1 μM of flgII-28, or buffer alone for 2 min before harvesting. Total protein was extracted from 500 mg of *N. benthamiana* leaves in 1.5 mL of extraction buffer consisting of 50 mM of Tris-HCl at pH 7.5, 150 mM of NaCl, 0.5% Triton X-100, 1% (v/v) plant protease inhibitor cocktail (Sigma-Aldrich), 1 mM of Na3VO4, 1 mM of NaF, and 20 mM of β-glycerophosphate. Soluble proteins were incubated with 20 μL of GFP-Trap_MA slurry (Chromotek) or anti-Myc magnetic beads (Thermo Fisher Scientific) per sample for 2 h at 4°C, followed by washing three times with cold extraction buffer, and one more wash with cold 50 mM of Tris-HCl at pH 7.5. Proteins were eluted with 40-μL 2× Laemmli sample buffer and boiled at 95°C for 5 min. For input samples, 8-μL soluble protein mixed with 2× sample buffer was loaded for gel electrophoresis. Proteins were loaded on 8% SDS-PAGE gel, blotted on PVDF membrane (Merck Millipore), treated with appropriate antibodies, and detected by Immobilon Forte western HRP substrate (Millipore Sigma).

RT-qPCR

Four leaflets from the third leaf of 5-week-old plants were first syringe-infiltrated with 1 μM of flgII-28 or buffer. Three plants were used for each treatment and two biological replicates were performed. Leaf tissues were collected 0.5, 1, 2, 4, 6, and 8 h after infiltration, immediately frozen in liquid N_2 and stored at −80°C until used. Total RNA was isolated using an RNeasy Plant Mini Kit (Qiagen). RNA (4 μg) was treated with TURBO DNA-free DNase (Thermo Fisher Scientific) twice, each for 30 min at 37°C. First-strand complementary DNA was synthesized from 2 μg of RNA using SuperScript III (Thermo Fisher Scientific). Quantitative PCR was performed with specific primers (Supplemental Table S1) using the QuantStudio 6 Flex Real-Time PCR System (Thermo Fisher Scientific) and cycling conditions for PCR were 50°C for

2 min, 95°C for 10 min, and then 40 cycles of 95°C for 30 s, 56°C for 30 s, and 72°C for 30 s.

Accession Numbers

Sequence data from this article can be found in the Plant Genome Editing Database (http://plantcrispr.org) under Solyc09g014720.

Supplemental Data

The following supplemental materials are available.

Supplemental Figure S1. The growth, development, and morphology of Wak1 plants was indistinguishable from wild-type RG-PtoR tomato plants.

Supplemental Figure S2. Enhanced susceptibility to DC3000ΔΔ cosegregates with the *Wak1* mutations.

Supplemental Figure S3. The Δwak1 plants are not affected in flg22 or flgII-28-induced ROS production.

Supplemental Figure S4. The Δwak1 plants are not affected in csp22-induced ROS production.

Supplemental Figure S5. Wak1 associates with Fls2 independently of flg22.

Supplemental Table S1. Primers used in this study.

ACKNOWLEDGMENTS

We thank Robyn Roberts for comments on the article and for sharing seeds of the Δfls2.1/2.2/3 line, Holly M. Roberts for assistance with vacuum infiltration and sequencing of the F2 populations, Brian Bell and Jay Miller for plant care, Joyce Van Eck for tomato transformation, and Diana Lauff for assisting with experiments involving microscopy.

Received February 6, 2020; accepted April 29, 2020; published May 5, 2020.

LITERATURE CITED

Anderson CM, Wagner TA, Perret M, He ZH, He D, Kohorn BD (2001) WAKs: Cell wall-associated kinases linking the cytoplasm to the extracellular matrix. Plant Mol Biol **47:** 197–206

Bacete L, Mélida H, Miedes E, Molina A (2018) Plant cell wall-mediated immunity: Cell wall changes trigger disease resistance responses. Plant J **93:** 614–636

Bae S, Park J, Kim JS (2014) Cas-OFFinder: A fast and versatile algorithm that searches for potential off-target sites of Cas9 RNA-guided endonucleases. Bioinformatics **30:** 1473–1475

Bigeard J, Colcombet J, Hirt H (2015) Signaling mechanisms in pattern-triggered immunity (PTI). Mol Plant **8:** 521–539

Boller T, Felix G (2009) A renaissance of elicitors: Perception of microbe-associated molecular patterns and danger signals by pattern-recognition receptors. Annu Rev Plant Biol **60:** 379–406

Brinkman EK, Chen T, Amendola M, van Steensel B (2014) Easy quantitative assessment of genome editing by sequence trace decomposition. Nucleic Acids Res **42:** e168

Brutus A, Sicilia F, Macone A, Cervone F, De Lorenzo G (2010) A domain swap approach reveals a role of the plant wall-associated kinase 1 (WAK1) as a receptor of oligogalacturonides. Proc Natl Acad Sci USA **107:** 9452–9457

Chandra S, Martin GB, Low PS (1996) The Pto kinase mediates a signaling pathway leading to the oxidative burst in tomato. Proc Natl Acad Sci USA **93:** 13393–13397

Chinchilla D, Zipfel C, Robatzek S, Kemmerling B, Nürnberger T, Jones JD, Felix G, Boller T (2007) A flagellin-induced complex of the receptor FLS2 and BAK1 initiates plant defence. Nature **448:** 497–500

Cui H, Tsuda K, Parker JE (2015) Effector-triggered immunity: From pathogen perception to robust defense. Annu Rev Plant Biol **66:** 487–511

Delteil A, Gobbato E, Cayrol B, Estevan J, Michel-Romiti C, Dievart A, Kroj T, Morel JB (2016) Several wall-associated kinases participate positively and negatively in basal defense against rice blast fungus. BMC Plant Biol **16:** 17

Dmochowska-Boguta M, Kloc Y, Zielezinski A, Werecki P, Nadolska-Orczyk A, Karlowski WM, Orczyk W (2020) TaWAK6 encoding wall-associated kinase is involved in wheat resistance to leaf rust similar to adult plant resistance. PLoS One **15:** e0227713

Gramegna G, Modesti V, Savatin DV, Sicilia F, Cervone F, De Lorenzo G (2016) GRP-3 and KAPP, encoding interactors of WAK1, negatively affect defense responses induced by oligogalacturonides and local response to wounding. J Exp Bot **67:** 1715–1729

Harkenrider M, Sharma R, De Vleesschauwer D, Tsao L, Zhang X, Chern M, Canlas P, Zuo S, Ronald PC (2016) Overexpression of rice wall-associated kinase 25 (OsWAK25) alters resistance to bacterial and fungal pathogens. PLoS One **11:** e0147310

Hind SR, Strickler SR, Boyle PC, Dunham DM, Bao Z, O'Doherty IM, Baccile JA, Hoki JS, Viox EG, Clarke CR, et al (2016) Tomato receptor FLAGELLIN-SENSING 3 binds flgII-28 and activates the plant immune system. Nat Plants **2:** 16128

Hou X, Tong H, Selby J, Dewitt J, Peng X, He ZH (2005) Involvement of a cell wall-associated kinase, WAKL4, in Arabidopsis mineral responses. Plant Physiol **139:** 1704–1716

Hu K, Cao J, Zhang J, Xia F, Ke Y, Zhang H, Xie W, Liu H, Cui Y, Cao Y, et al (2017) Improvement of multiple agronomic traits by a disease resistance gene via cell wall reinforcement. Nat Plants **3:** 17009

Hu W, Lv Y, Lei W, Li X, Chen Y, Zheng L, Xia Y, Shen Z (2014) Cloning and characterization of the *Oryza sativa* wall-associated kinase gene OsWAK11 and its transcriptional response to abiotic stresses. Plant Soil **384:** 335–346

Hurni S, Scheuermann D, Krattinger SG, Kessel B, Wicker T, Herren G, Fitze MN, Breen J, Presterl T, Ouzunova M, et al (2015) The maize disease resistance gene Htn1 against northern corn leaf blight encodes a wall-associated receptor-like kinase. Proc Natl Acad Sci USA **112:** 8780–8785

Jacobs TB, Zhang N, Patel D, Martin GB (2017) Generation of a collection of mutant tomato lines using pooled CRISPR libraries. Plant Physiol **174:** 2023–2037

Jia Y, Martin GB (1999) Rapid transcript accumulation of pathogenesis-related genes during an incompatible interaction in bacterial speck disease-resistant tomato plants. Plant Mol Biol **40:** 455–465

Jiang F, Doudna JA (2017) CRISPR-Cas9 structures and mechanisms. Annu Rev Biophys **46:** 505–529

Jones JB (1991) Bacterial speck. In JB Jones, JP Jones, RE Stall, and TA Zitter, eds, Compendium of Tomato Diseases. APS Press, St. Paul, MN, pp 26–27

Jubic LM, Saile S, Furzer OJ, El Kasmi F, Dangl JL (2019) Help wanted: Helper NLRs and plant immune responses. Curr Opin Plant Biol **50:** 82–94

Kearse M, Moir R, Wilson A, Stones-Havas S, Cheung M, Sturrock S, Buxton S, Cooper A, Markowitz S, Duran C, et al (2012) Geneious Basic: An integrated and extendable desktop software platform for the organization and analysis of sequence data. Bioinformatics **28:** 1647–1649

Kimura S, Sinha N (2008) Tomato (*Solanum lycopersicum*): A model fruit-bearing crop. CSH Protoc **2008:** pdb emo105

Kohorn BD, Johansen S, Shishido A, Todorova T, Martinez R, Defeo E, Obregon P (2009) Pectin activation of MAP kinase and gene expression is WAK2 dependent. Plant J **60:** 974–982

Kohorn BD, Kobayashi M, Johansen S, Riese J, Huang LF, Koch K, Fu S, Dotson A, Byers N (2006) An Arabidopsis cell wall-associated kinase required for invertase activity and cell growth. Plant J **46:** 307–316

Lally D, Ingmire P, Tong HY, He ZH (2001) Antisense expression of a cell wall-associated protein kinase, WAK4, inhibits cell elongation and alters morphology. Plant Cell **13:** 1317–1331

Li B, Meng X, Shan L, He P (2016) Transcriptional regulation of pattern-triggered immunity in plants. Cell Host Microbe **19:** 641–650

Li H, Zhou SY, Zhao WS, Su SC, Peng YL (2009) A novel wall-associated receptor-like protein kinase gene, OsWAK1, plays important roles in rice blast disease resistance. Plant Mol Biol **69:** 337–346

Lolle S, Stevens D, Coaker G (2020) Plant NLR-triggered immunity: From receptor activation to downstream signaling. Curr Opin Immunol **62:** 99–105

Lou HQ, Fan W, Jin JF, Xu JM, Chen WW, Yang JL, Zheng SJ (2019) A NAC-type transcription factor confers aluminium resistance by

regulating cell wall-associated receptor kinase 1 and cell wall pectin. Plant Cell Environ **43:** 463–478

Martin GB (2012) Suppression and activation of the plant immune system by *Pseudomonas syringae* effectors AvrPto and AvrPtoB. In F Martin, and S Kamoun, eds, Effectors in Plant-Microbe Interactions. Wiley-Blackwell, Ames, IA, pp 123–154

Martin GB, Bogdanove AJ, Sessa G (2003) Understanding the functions of plant disease resistance proteins. Annu Rev Plant Biol **54:** 23–61

Martin GB, Brommonschenkel SH, Chunwongse J, Frary A, Ganal MW, Spivey R, Wu T, Earle ED, Tanksley SD (1993) Map-based cloning of a protein kinase gene conferring disease resistance in tomato. Science **262:** 1432–1436

Melotto M, Underwood W, He SY (2008) Role of stomata in plant innate immunity and foliar bacterial diseases. Annu Rev Phytopathol **46:** 101–122

Melotto M, Underwood W, Koczan J, Nomura K, He SY (2006) Plant stomata function in innate immunity against bacterial invasion. Cell **126:** 969–980

Melotto M, Zhang L, Oblessuc PR, He SY (2017) Stomatal defense a decade later. Plant Physiol **174:** 561–571

Murray MG, Thompson WF (1980) Rapid isolation of high molecular weight plant DNA. Nucleic Acids Res **8:** 4321–4325

Nguyen HP, Chakravarthy S, Velásquez AC, McLane HL, Zeng L, Nakayashiki H, Park D-H, Collmer A, Martin GB (2010) Methods to study PAMP-triggered immunity using tomato and *Nicotiana benthamiana*. Mol Plant Microbe Interact **23:** 991–999

Pedley KF, Martin GB (2003) Molecular basis of Pto-mediated resistance to bacterial speck disease in tomato. Annu Rev Phytopathol **41:** 215–243

Pombo MA, Zheng Y, Fei Z, Martin GB, Rosli HG (2017) Use of RNA-seq data to identify and validate RT-qPCR reference genes for studying the tomato-Pseudomonas pathosystem. Sci Rep **7:** 44905

Rosli HG, Zheng Y, Pombo MA, Zhong S, Bombarely A, Fei Z, Collmer A, Martin GB (2013) Transcriptomics-based screen for genes induced by flagellin and repressed by pathogen effectors identifies a cell wall-associated kinase involved in plant immunity. Genome Biol **14:** R139

Saintenac C, Lee WS, Cambon F, Rudd JJ, King RC, Marande W, Powers SJ, Bergès H, Phillips AL, Uauy C, et al (2018) Wheat receptor-kinase-like protein Stb6 controls gene-for-gene resistance to fungal pathogen *Zymoseptoria tritici*. Nat Genet **50:** 368–374

Salmeron JM, Oldroyd GE, Rommens CM, Scofield SR, Kim HS, Lavelle DT, Dahlbeck D, Staskawicz BJ (1996) Tomato *Prf* is a member of the leucine-rich repeat class of plant disease resistance genes and lies embedded within the *Pto* kinase gene cluster. Cell **86:** 123–133

Shi G, Zhang Z, Friesen TL, Raats D, Fahima T, Brueggeman RS, Lu S, Trick HN, Liu Z, Chao W, et al (2016) The hijacking of a receptor kinase-driven pathway by a wheat fungal pathogen leads to disease. Sci Adv **2:** e1600822

Stegmann M, Monaghan J, Smakowska-Luzan E, Rovenich H, Lehner A, Holton N, Belkhadir Y, Zipfel C (2017) The receptor kinase FER is a RALF-regulated scaffold controlling plant immune signaling. Science **355:** 287–289

Sun Y, Li L, Macho AP, Han Z, Hu Z, Zipfel C, Zhou JM, Chai J (2013) Structural basis for flg22-induced activation of the Arabidopsis FLS2-BAK1 immune complex. Science **342:** 624–628

Tamborski J, Krasileva KV (2020) Evolution of plant NLRs: From natural history to precise modifications. Annu Rev Plant Biol **71:** 35901

Toruño TY, Stergiopoulos I, Coaker G (2016) Plant-pathogen effectors: Cellular probes interfering with plant defenses in spatial and temporal manners. Annu Rev Phytopathol **54:** 419–441

Voigt CA (2014) Callose-mediated resistance to pathogenic intruders in plant defense-related papillae. Front Plant Sci **5:** 168

Wagner TA, Kohorn BD (2001) Wall-associated kinases are expressed throughout plant development and are required for cell expansion. Plant Cell **13:** 303–318

Wei HL, Zhang W, Collmer A (2018) Modular study of the type III effector repertoire in *Pseudomonas syringae* pv. tomato DC3000 reveals a matrix of effector interplay in pathogenesis. Cell Rep **23:** 1630–1638

Xiang T, Zong N, Zou Y, Wu Y, Zhang J, Xing W, Li Y, Tang X, Zhu L, Chai J, et al (2008) *Pseudomonas syringae* effector AvrPto blocks innate immunity by targeting receptor kinases. Curr Biol **18:** 74–80

Yang K, Qi L, Zhang Z (2014) Isolation and characterization of a novel wall-associated kinase gene TaWAK5 in wheat (*Triticum aestivum*). Crop J **2:** 255–266

Yang P, Praz C, Li B, Singla J, Robert CAM, Kessel B, Scheuermann D, Lüthi L, Ouzunova M, Erb M, et al (2019) Fungal resistance mediated by maize wall-associated kinase ZmWAK-RLK1 correlates with reduced benzoxazinoid content. New Phytol **221:** 976–987

Zhang N, Roberts HM, Van Eck J, Martin GB (2020) Generation and molecular characterization of CRISPR/Cas9-induced mutations in 63 immunity-associated genes in tomato reveals specificity and a range of gene modifications. Front Plant Sci **11:** 10

Zheng Y, Jiao C, Sun H, Rosli HG, Pombo MA, Zhang P, Banf M, Dai X, Martin GB, Giovannoni JJ, et al (2016) iTAK: A program for genome-wide prediction and classification of plant transcription factors, transcriptional regulators, and protein kinases. Mol Plant **9:** 1667–1670

Zipfel C (2014) Plant pattern-recognition receptors. Trends Immunol **35:** 345–351

Zuo W, Chao Q, Zhang N, Ye J, Tan G, Li B, Xing Y, Zhang B, Liu H, Fengler KA, et al (2015) A maize wall-associated kinase confers quantitative resistance to head smut. Nat Genet **47:** 151–157